



Published in final edited form as:

*Adv Funct Mater.* 2013 March 6; 23(9): 1111–1119. doi:10.1002/adfm.201201922.

## pH-Based Regulation of Hydrogel Mechanical Properties Through Mussel-Inspired Chemistry and Processing

**Dr. Devin G. Barrett,**

Biomedical Engineering Department Chemistry of Life Processes Institute Institute for Bionanotechnology in Medicine Northwestern University Evanston, IL 60208, USA

**Dr. Dominic E. Fullenkamp,**

Biomedical Engineering Department Chemistry of Life Processes Institute Northwestern University Evanston, IL 60208, USA

**Dr. Lihong He,**

Biomedical Engineering Department Chemistry of Life Processes Institute Northwestern University Evanston, IL 60208, USA

**Dr. Niels Holten-Andersen,**

Chemistry Department Institute for Biophysical Dynamics James Franck Institute University of Chicago Chicago, IL 60637, USA

**Prof. Ka Yee C. Lee, and**

Chemistry Department Institute for Biophysical Dynamics James Franck Institute University of Chicago Chicago, IL 60637, USA

**Prof. Phillip B. Messersmith\***

Biomedical Engineering Department Materials Science and Engineering Department Chemical and Biological Engineering Department Chemistry of Life Processes Institute Institute for Bionanotechnology in Medicine Robert H. Lurie Comprehensive Cancer Center Northwestern University Evanston, IL 60208, USA

### Abstract

The mechanical holdfast of the mussel, the byssus, is processed at acidic pH yet functions at alkaline pH. Byssi are enriched in  $\text{Fe}^{3+}$  and catechol-containing proteins, species with chemical interactions that vary widely over the pH range of byssal processing. Currently, the link between pH,  $\text{Fe}^{3+}$ -catechol reactions, and mechanical function are poorly understood. Herein, we describe how pH influences the mechanical performance of materials formed by reacting synthetic catechol polymers with  $\text{Fe}^{3+}$ . Processing  $\text{Fe}^{3+}$ -catechol polymer materials through a mussel-mimetic acidic-to-alkaline pH change leads to mechanically tough materials based on a covalent network fortified by sacrificial  $\text{Fe}^{3+}$ -catechol coordination bonds. Our findings offer the first direct evidence of  $\text{Fe}^{3+}$ -induced covalent cross-linking of catechol polymers, reveal additional insight into the pH dependence and mechanical role of  $\text{Fe}^{3+}$ -catechol interactions in mussel byssi, and illustrate the wide range of physical properties accessible in synthetic materials through mimicry of mussel protein chemistry and processing.

### Keywords

Biomimetics; Hydrogels; Polymeric Materials; Structure-Property Relationships

---

\*<sup>1</sup>philm@northwestern.edu.

## 1. Introduction

Load-bearing biological materials serve as valuable models for designing synthetic materials with extraordinary mechanical properties.<sup>[1-3]</sup> This process often begins with observations of interesting physical properties of tissues followed by identification of essential elements or building blocks. However, biologically inspired design is most enabling when there exists an understanding of basic chemical and physical principles underlying structure-function relationships, including tissue processing/fabrication strategies in biological systems.<sup>[4-6]</sup> Spider dragline silk and mussel byssi are two examples of fibrous biological tissues with overtly mechanical functions that have attracted great interest among researchers due to their exceptional material properties and vast potential for applications.<sup>[7,8]</sup> In the case of spider silk, the protein building blocks were described many years before key features of silk fiber spinning were known.<sup>[9-11]</sup> One recently uncovered feature of silk fiber processing is the apparent acidification of the duct lumen during spinning,<sup>[12]</sup> which is believed to play a role in protein condensation, assembly and fiber formation from soluble precursors.<sup>[13,14]</sup>

pH regulation is also employed by marine organisms during secretion of attachment structures.<sup>[15]</sup> The mussel byssus is a proteinaceous and acellular holdfast composed of a collection of byssal threads tethering the organism to a surface. Many mussel species inhabit turbulent intertidal zones by relying on byssal threads that are strong, resilient, and designed to resist damage and detachment.<sup>[16-21]</sup> The byssus is molded from liquid protein precursors whose pH during early secretion is initially acidic (pH  $\approx$  5.8);<sup>[22]</sup> after formation of the byssus and exposure to sea water, the adhesive structure equilibrates to marine pH ( $\sim$ 8.5). While the byssus is primarily composed of organic macromolecules, it has been shown to be enriched in inorganic elements such as Fe<sup>3+</sup>,<sup>[23]</sup> and its remarkable mechanical properties have been hypothesized to originate from both inorganic (metal coordination) and organic (covalent) bonds.<sup>[19-21,24]</sup> For example, the ability of the byssus to ‘self-heal’ after suffering apparently non-recoverable mechanical deformation<sup>[19]</sup> is thought to be related to coordination bonds formed between metals and byssal proteins.<sup>[20,21,24]</sup> Although there is a growing effort to develop synthetic materials inspired by mussel byssal proteins and threads,<sup>[8,25-28]</sup> mimicry of mussel byssal processing is still in the early stages.<sup>[29-31]</sup>

The complex mechanochemical interactions between Fe<sup>3+</sup> and catechols during and after byssal formation are the particular focus of this work. The catechol-containing residue 3,4-dihydroxy-L-phenylalanine (DOPA) is found in most byssal proteins, and previous studies have shown that Fe<sup>3+</sup>-catechol coordination interactions are mechanically active.<sup>[24,30,32-34]</sup> While multiple reports have recently compared gels cross-linked by oxidative covalent coupling and catechol coordination of Fe<sup>3+</sup>, the interplay between these curing mechanisms is poorly understood.<sup>[30,34]</sup> This topic should be further investigated due to the complex interactions between Fe<sup>3+</sup> and catechols; spectroscopic evidence has linked the presence of Submitted to Fe<sup>3+</sup> to catechol oxidation,<sup>[35,36]</sup> and speculation exists about the possible involvement of Fe<sup>3+</sup> in formation of covalent DOPA-DOPA linkages.<sup>[37]</sup>

In this report, we show that reactions between Fe<sup>3+</sup> and catechol polymers are strongly dependent upon pH, with covalent catechol-catechol linkages and Fe<sup>3+</sup>-catechol coordination dominating at acidic and basic conditions, respectively. The mechanical effects of such diverse reaction products were studied in model polymer hydrogels by using pH to regulate the balance of covalent and coordination bonds in, and therefore the viscoelastic character of, the gel network. Finally, mimicking the acidic-to-basic pH switch that occurs during byssus formation in our synthetic system led to covalent gel networks mechanically augmented by Fe<sup>3+</sup>-catechol coordination bonds. In these networks, Fe<sup>3+</sup>-catechol coordination bonds dissipate energy through rupture but rapidly re-form to regenerate the original mechanical properties during subsequent loading cycles, functioning as sacrificial

bonds in analogy to those that are such prominent features of structural biological tissues.<sup>[38,39]</sup>

## 2. Cross-Linking of Monofunctional Catechol Polymers: Influence of $[\text{Fe}^{3+}]$ and pH

We first investigated the interactions between  $\text{Fe}^{3+}$  and a monofunctional catechol-containing polymer (mPEG-cat; ~ 5 kDa; Figure 1) in order to understand the impact of pH and  $\text{Fe}^{3+}$ :catechol stoichiometry on the formation of covalent polymerization products. The use of mPEG-cat allowed gel permeation chromatography (GPC) experiments to be performed with similar end-group concentrations and buffer conditions used for gel studies (described below), but without the complications associated with network formation. As shown in Figure 1, at pH 3, GPC traces reveal increased multimer formation, with a linear dependence on the  $\text{Fe}^{3+}$ :catechol ratio (Supplementary Figure S1a). At pH 3 and a  $\text{Fe}^{3+}$ :catechol ratio of 3:3, the reaction is complete after 1 h, and reaction mixtures contained ~30 % multimers, with the dominant species being the mPEG-cat dimer (Figure 1 and Supplementary Figure S1b).

GPC studies of mPEG-cat with  $\text{Fe}^{3+}$  at pH 5 revealed a surprisingly high degree of mPEG-cat polymerization after 24 h (Figure 1; Supplementary Figure S1). This result was unexpected, as visual inspection of a mixture of the polyfunctional, catechol-containing 8cPEGa – 8-arm, catechol-modified PEG with amide linkages – (Figure 2) with  $\text{Fe}^{3+}$  under similar conditions revealed no gel formation, as determined by vial inversion. We also found that the reaction at pH 5 was not significantly dependent on the  $\text{Fe}^{3+}$ :catechol ratio, as the sample with a ratio of 1:3 produced an essentially equivalent amount of multimers as the sample with a ratio of 3:3. Interestingly, the time-dependence of the reaction at pH 5 (Figure S1b) showed that polymerization occurred slowly and only resulted in significant multimer formation after several hours. GPC results for reactions at pH 7 were qualitatively similar to pH 5, although the cross-linking reaction appeared to be slower. After 24 h of reaction at pH 7, all mPEG-cat solutions with  $\text{Fe}^{3+}$  contained ~10 % multimer, compared to ~25-30 % for reactions at pH 5. From these data, we can say that the extent and rate of covalent polymerization of catechols by  $\text{Fe}^{3+}$  are highest at low pH and decrease as neutral pH is approached.

GPC results at pH 9 were unique because of the significant presence of multimers after 24 h in the absence of  $\text{Fe}^{3+}$ , a result we attribute to the auto-oxidation of catechols in basic conditions. Multimer formation at pH 9 proceeded slowly and decreased as the  $\text{Fe}^{3+}$ :catechol ratio increased (Figure 1 and Supplementary Figure S1). The inverse relationship between multimer formation and  $\text{Fe}^{3+}$ :catechol ratio suggests that  $\text{Fe}^{3+}$  serves a protective role against auto-oxidation of catechols at basic pH,<sup>[40]</sup> though we cannot exclude a minor suppression of auto-oxidation as a result of the slight acidification associated with added  $\text{Fe}^{3+}$  (the strong acidity of  $\text{FeCl}_3$  slightly depressed the pH of the buffered reaction solutions; see Supplementary Table S1).

mPEG-cat was also used to study the presence of coordination bonds by UV-Vis spectroscopy, the standard method of characterizing these linkages. The interactions between catechols and  $\text{Fe}^{3+}$  are known to produce signature colors as a function of pH.<sup>[30]</sup> When  $\text{Fe}^{3+}$  and mPEG-cat (molar ratio of 2:3) were combined at pH 3, 5, 7, and 9, the solutions became green, blue, purple, and red (Supplementary Figure S2). These results correspond well to the coordination-based hydrogels described by Holten-Andersen and colleagues.<sup>[30]</sup> Further, in anticipation of novel hydrogels to be designed later, we incubated  $\text{Fe}^{3+}$  and mPEG-cat (molar ratio of 2:3) at pH 3 for 2 h; during this time, the samples turned green, as expected. These solutions were then subjected to an increase in alkalinity to pH 7 or 9; again, these samples changed colors to purple or red, respectively. An adjustment to pH 5 was not possible due to the inability to overwhelm the pH 3 buffer without overly

diluting the coordinating species. Taken together, these results suggest that catechol systems are able to coordinate  $\text{Fe}^{3+}$  at elevated pH, including after a period of covalent oligomerization in acidic conditions.

### 3. Properties of Catechol Polymer Gels: Influence of $[\text{Fe}^{3+}]$ and pH

$\text{Fe}^{3+}$ -induced gel formation of a polyfunctional, catechol-terminated PEG (8cPEGa) was characterized both as a function of pH and  $\text{Fe}^{3+}$ :catechol ratio. As demonstrated in Supplementary Figure S3, covalent gels rapidly formed (<1 min) in unbuffered water (pH ~2) at  $\text{Fe}^{3+}$ :catechol ratio of 2:3. These hydrogels appear to be elastic solids, with  $G'$  and  $G''$  displaying essentially frequency-independent behavior and  $G' \gg G''$ . The mechanical properties are similar in modulus and yield strain to other catechol-modified PEG hydrogels formed by covalent cross-linking with  $\text{NaIO}_4$ .<sup>[27,41]</sup> The ability of  $\text{Fe}^{3+}$  to rapidly oxidize and covalently cross-link these polymers at low pH is consistent with our GPC studies (Figure 1). Hydrogels also formed at  $\text{Fe}^{3+}$ :catechol ratio of 3:3, though these gels formed too rapidly to be inserted into our rheometer prior to gelation. Solutions with  $\text{Fe}^{3+}$ :catechol of 1:3 in unbuffered water did not form gels (Supplementary Figure S3), likely due to insufficient cross-linking for network percolation.

Next, we studied gel formation in buffered systems in order to probe hydrogel mechanical properties as a function of pH and  $\text{Fe}^{3+}$ :catechol ratio. Supplementary Table S2 documents gelation times at various cross-linking conditions. As judged by vial inversion, gels formed slower at acidic pH compared to those cross-linked at alkaline pH. While gels did not form within 60 min at pH 5, these solutions immediately became more viscous upon mixing 8cPEGa and  $\text{Fe}^{3+}$ .

To differentiate between covalent- and coordination-based cross-linking, gels were further studied by rheology. Gels did not form at pH 3 for a  $\text{Fe}^{3+}$ :catechol ratio of 1:3. For larger  $\text{Fe}^{3+}$ :catechol ratios, we see mechanical properties that are typical of elastic solids and similar to gels formed in unbuffered water (Figure 2 and Supplementary Figure S4). Step-strain measurements show the relaxation time to be essentially infinite, consistent with a covalently gelled network. Additionally, the modulus of gels formed at pH 3 increased at higher  $\text{Fe}^{3+}$ :catechol ratios, which is consistent with a higher cross-linking density.

At pH 9, materials displaying Maxwell-like relaxation behavior were formed in the presence of  $\text{Fe}^{3+}$ . This behavior reflects coordination cross-linking, likely in a bis- or tris-catecholate configuration, and is consistent with the previous report of Holten-Andersen *et al.*<sup>[30]</sup> Interestingly, gels formed with a  $\text{Fe}^{3+}$ :catechol ratio of 3:3 were stiffer at high frequency than those formed with a ratio of 1:3 or 2:3. This result is not intuitive, as one would expect equimolar amounts of  $\text{Fe}^{3+}$  and catechol end-groups to soften the gel by forming the mono-catecholate species, thus preventing coordination-based cross-linking that must proceed through bis- and tris-catecholate motifs.

Hydrogels formed at pH values between 5 and 7 displayed very different material properties. As shown in Figure 2, gels formed at pH 5 are simply viscous liquids with relatively short relaxation times; this observation is in stark contrast to both the essentially infinite relaxation times of covalent gels formed at pH 3 and the Maxwell-like behavior of coordination-dominated gels formed at pH 9. At pH 7, unexpected material properties were observed. As demonstrated by past equilibrium titration studies of  $\text{Fe}^{3+}$ -catechol solutions<sup>[40]</sup> and our own GPC studies, neither covalent nor coordination cross-linking is expected to be especially dominant at pH 7.  $\text{Fe}^{3+}$ -mediated oxidative oligomerization is not very efficient at pH 7, and a significant fraction of terminal catechols are not expected to participate in network formation through coordination of  $\text{Fe}^{3+}$ . However, surprisingly rigid materials resulted when gels were formed at pH 7. Not only were the moduli of gels formed

at pH 7 greater than those of materials at pH 9, gel relaxation times under these conditions are clearly longer than those formed at pH 9, as no crossover is seen in the frequency sweep at pH 7 (Figure 2). We are currently investigating why pH 7 gels have significantly longer relaxation times than pH 9 gels. We hypothesize that the higher hydroxide concentration at pH 9 may be increasing the bond relaxation rate, though a role for the buffer or the amount of covalent cross-linking cannot be ruled out at this time. In order to further investigate the balance of covalent and coordination bonds in these materials, their stabilities in solutions of ethylenediaminetetraacetic acid (EDTA) was monitored (Supplementary Figure S5, Supplementary Table S3). Samples designed at pH 3 were stable to EDTA, while hydrogels fabricated at pH 5, 7, and 9 almost entirely dissolved when exposed to EDTA. These data qualitatively support our interpretation of rheological data.

Taken together, these results suggest that covalent cross-linking plays a very significant role at pH 3 and a lesser role at pH 5, 7, and 9. To the best of our knowledge, our GPC results showing mPEG-cat multimers are the first direct evidence of oxidative catechol oligomerization by  $\text{Fe}^{3+}$ . Though no direct evidence of this reaction has been previously described, spectroscopic results have shown that catechols can be oxidized to the *o*-quinone form by  $\text{Fe}^{3+}$ .<sup>[35,36]</sup> Additionally, a hypothesis that  $\text{Fe}^{3+}$  serves as an inorganic oxidant leading to byssal protein cross-linking has been proposed.<sup>[37]</sup> Our GPC experiments, albeit using a fully synthetic model polymer, support this hypothesis and provide the first direct evidence of covalent reaction products. These findings warrant further studies as to whether or not  $\text{Fe}^{3+}$ , which is enriched in mussel adhesives relative to seawater,<sup>[42]</sup> acts as an inorganic oxidant for formation of byssal threads.

#### 4. Mimicking the pH increase of byssal processing

As previously stated, during byssal processing, liquid protein precursors are secreted at acidic pH<sup>[22]</sup> and rapidly equilibrate to alkaline marine pH (~8.5) when exposed to seawater. Motivated in part by the use of pH regulation by the mussel and our findings that show pH-dependent  $\text{Fe}^{3+}$ -catechol interactions, we sought to create functional materials that exhibit exceptional mechanical properties through mussel-inspired pH processing. Thus,  $\text{Fe}^{3+}$ -catechol polymer hydrogels were formed for 24 h at pH 3 with an  $\text{Fe}^{3+}$ :catechol ratio of 2:3, and then immersed for 24 h in buffer at pH 3, 5, 7 or 9. The first step of this approach imparted an initial and equivalent covalent network in all samples, allowing us to then probe the mechanical contribution of  $\text{Fe}^{3+}$ -catechol coordination bonds that are expected to occur upon equilibration at higher pH.

In the first experiment, hydrogels were strained in compression by 5, 10, or 20 % and the evolution of stress was monitored for 100 s (Figure 3, Supplementary Figure S6). The discussion here will focus on samples strained at 20 %, however the trends mirror those observed at 5 % and 10 % strain as indicated in Supplementary Table S4. The modulus, amount of relaxation, and relaxation rate, were strongly dependent on equilibration pH. Extraction of the initial and steady state moduli from the relaxation curves revealed an increase in modulus with increasing pH (Figure 4). Hydrogels equilibrated at pH 3, 5, 7, and 9 dissipated 3.3 %, 9.7 %, 32.3 %, and 51.2 % of the maximum stress, respectively. The relaxation times were calculated to be approximately 25 s for pH 5, 18 s for pH 7, and 5 s for pH 9 (Figure 4); no relaxation times were determined for materials equilibrated at pH 3 due to the presence of a primarily covalent gel network.

In the second experiment, samples were cycled through compression loops with increasing strain (10 %, 20 %, 40 %, 60 %, 70 %, 80 %), allowing us to monitor the effect of equilibration pH on mechanical recovery (Figure 5). A qualitative trend observed in these data was the increase in compression modulus with increasing equilibration pH, which was consistent with the results of stress relaxation experiments (Figure 4) and can be attributed



to augmentation of the covalent network by Fe<sup>3+</sup>-catechol coordination bonds, which are much more prevalent at high pH. Notably, gels equilibrated at pH 9 sustained the largest stress (~260 kPa) and strain values (80 %) without suffering permanent damage. A prominent feature in the compression loops was the presence of hysteresis between loading and unloading curves. Minimal hysteresis was observed for gels equilibrated at pH 3 and 5. However, substantial hysteresis was observed in samples equilibrated at pH 7 and 9, reflecting energy dissipation by rupture of Fe<sup>3+</sup>-catechol coordination bonds. Presumably, ruptured coordination bonds rapidly re-form, as the loading curves from successive compression loops with increasing strain were nearly perfectly overlapping (Figure 5).

Covalently cross-linked hydrogels are essentially Hookean elastic materials at low strains, acting like springs that store energy without dissipation. Fe<sup>3+</sup>-catechol gels equilibrated at pH 3 fit this description due to their purely covalent nature (no Fe<sup>3+</sup>-catechol coordination bonds should form at such acidic pH). In contrast, the relaxation and hysteresis observed in gels equilibrated at pH 7 and 9 are attributed to the presence of mechanically functional Fe<sup>3+</sup>-catechol coordination bonds (Figure 5, Scheme 1). Even at low strain, these gels displayed mechanical hysteresis between loading and unloading curves. Such viscoelastic behavior is reminiscent of the relaxation and hysteresis observed in recently reported synthetic muscle-mimetic biomaterials, which were designed to exhibit high toughness and resilience reminiscent of native tissues by incorporating secondary and tertiary structures that dissipate energy under applied force.<sup>[43]</sup> This viscoelasticity is also a characteristic feature of biological materials like tendon and cartilage,<sup>[38,39]</sup> where it plays an important role in transferring and mitigating loads between soft and hard tissues.

Noncovalent interactions within and between macromolecular constituents often play key roles in defining the mechanical properties of biological tissues.<sup>[19-21,24,44-47]</sup> For example, noncovalent interactions act in a sacrificial manner under applied loads by temporarily dissociating to dissipate energy and reveal hidden length, thereby enhancing toughness and preventing catastrophic material failure caused by the rupture of covalent bonds.<sup>[48]</sup> Because of their dynamic nature, such bonds can re-form to recover all or part of the original mechanical properties when the external load is removed.<sup>[19-21,44-46]</sup> Purely synthetic materials have been designed with covalent networks strengthened by noncovalent interactions such as hydrophobic bonds<sup>[49,50]</sup> and hydrogen bonding,<sup>[51-53]</sup> in an analogous way to achieve unique physical properties. Metal coordination interactions appear to have this function also, as illustrated here and by others.<sup>[30,54]</sup>

Finally, these experiments have revealed new details of Fe<sup>3+</sup>-catechol mechanochemistry, including direct demonstration of Fe<sup>3+</sup>-based oxidative oligomerization of catechols, the pH dependence of this reaction, and the mechanical consequences of covalent and coordination cross-links arising in Fe<sup>3+</sup>-containing catechol polymer systems. Our findings have important implications for understanding the processing and properties of the mussel byssus, with the conceptual scheme shown in Scheme 1 serving as a template for a more complete hypothesis on the mechanical function of Fe<sup>3+</sup> in mussel byssus. We postulate that co-secretion of Fe<sup>3+</sup> with DOPA-containing proteins, which occurs at acidic pH, gives rise to limited formation of a covalent network during byssus molding. Subsequent exposure to alkaline seawater increases the pH into the range where Fe<sup>3+</sup>-catechol coordination bonds are favored, and these bonds confer unique mechanical properties associated with their dynamic ability to rupture and re-form. Although the findings for the model polymer system reported herein support this dual role for Fe<sup>3+</sup>, further studies will be needed to examine if the mussel employs this mechanism for optimal mechanical performance of byssal threads.

## 5. Conclusions

This work demonstrates a new bio-inspired strategy for designing remarkably tough hydrogels. By regulating the pH of the reaction between catechol-terminated branched PEG and  $\text{Fe}^{3+}$ , a covalently cross-linked network was fortified with a series of coordination bonds, which act as sacrificial and reversible interactions to dissipate energy during deformation. With respect to opportunities related to the design of novel biologically inspired materials, our findings illustrate the richness of cross-linking chemistries and physical properties accessible in synthetic mussel-inspired materials, achieved through facile manipulation of pH, composition, and processing. Careful management of these variables affords access to a broad spectrum of physical properties reflecting the balance of covalent and coordination cross-linking in the gel network. These hydrogels, with a viscoelastic response and water content reminiscent of hydrated biological soft tissues, represent a novel class of mussel-mimetic biomaterials inspired in both content and processing.

## 6. Experimental

### Materials

Acetic acid, bicine, bis-Tris, bis-Tris hydrochloride, 3-(3,4-dihydroxyphenyl)propionic acid (DHPA), dichloromethane (DCM), dimethylformamide (DMF), ethylenediaminetetraacetic acid disodium salt dihydrate (EDTA), ferric chloride hexahydrate, formic acid, sodium acetate trihydrate, sodium formate, triethyleamine (TEA) were purchased from Sigma Aldrich (Milwaukee, WI). PEG products – linear monofunctional amine-terminated PEG (mPEG-NH<sub>3</sub>Cl; MW 5,000 g/mol) and 8-arm amine-terminated (8PEG-NH<sub>3</sub>Cl; hexaglycerin core; MW 20,000 g/mol) – were purchased from JenKem Technology USA Inc. (Allen, TX). N-hydroxybenzotriazole (HOBt) was purchased from Advanced ChemTech (Louisville, KY). 2-(1H-benzotriazole-1-yl)-1,1,3,3-tetramethyluronium hexafluorophosphate (HBTU) was purchased from EMD Chemicals (Gibbstown, NJ). All chemicals were used without further purification.

### Synthesis of mPEG-cat

Monofunctional, amine-terminated PEG (0.6 mmol, MW 5,000 g/mol) was dissolved in DCM (10 mL). To this solution, DHPA (1.2 mmol), HOBt (1.98 mmol), HBTU (1.2 mmol), and TEA (1.98 mmol) were sequentially added. Afterwards, DMF (5.0 mL) was added to help dissolve all reagents, and this coupling reaction was carried out at 20 °C under N<sub>2</sub> with continuous stirring for 2.0 h. The crude product was purified by precipitation in 300 mL of diethyl ether (1x) and in 300 mL of acidified methanol (3x) at -20 °C. After one additional precipitation in diethyl ether, mPEG-cat was dried under vacuum (~90 % conversion).

### Fe<sup>3+</sup>-Based Oligomerization of mPEG-cat as Studied by GPC

The reaction between mPEG-cat ( $M_n \sim 5,600$  Da by MALDI-TOF-MS) and  $\text{Fe}^{3+}$  was performed in buffered and unbuffered water. When the reaction was performed in unbuffered water, the pH was 2-3 due to the acidity of  $\text{FeCl}_3$ . Buffers (500 mM) of formate, acetate, bis-tris, and bicine were used to control the pH of solutions at pH 3, 5, 7, and 9, respectively. Aliquots of 3.0 mg mPEG-cat were dissolved into 7.14  $\mu\text{L}$  of water or buffer. Freshly prepared 100 mM, 200 mM, or 300 mM  $\text{FeCl}_3$  solutions (1.79  $\mu\text{L}$ ) was added to each solution of mPEG-cat to produce  $\text{Fe}^{3+}$ :catechol ratios of 1:3, 2:3, or 3:3, respectively. For 0x  $\text{Fe}^{3+}$  samples, 8.93  $\mu\text{L}$  of water or buffer was added to dissolve the polymer. The final reaction concentration of mPEG-cat was 60 mM (replicating the catechol concentration in gel studies). After 24 h, 6 h, or 1 h, 100 mM EDTA (10x EDTA relative to  $\text{Fe}^{3+}$ ) was added to the samples to sequester the  $\text{Fe}^{3+}$ . The samples were further diluted to 10 mg/mL with the GPC buffer (50 mM citrate, 100 mM NaSO<sub>4</sub>, pH 3.5). Each sample (10  $\mu\text{L}$ ) was

injected into an Agilent 1100 Series HPLC (flow rate 1.0 mL/min) equipped with a Shodex KW-803 GPC column (heated to 40 °C) and in line with Wyatt Dawn Heleos II and Optilab T-rEx dRI detectors. PEG standards (Varian) of 3,930, 7,920, 12,140, and 21,030 Da were prepared in GPC buffer at 10 mg/mL. Wyatt Astra software was used to calculate  $M_n$ ,  $M_w$ , and the relative percentages of monomer vs. multimer of mPEG-cat. The PEG dn/dc was taken to be 0.136 mL/g.

### UV-Vis Spectroscopy with mPEG-cat and Fe<sup>3+</sup>

UV-Vis data were recorded on a Shimadzu BioSpec-nano spectrophotometer. mPEG-cat was dissolved in buffer (pH 3, 5, 7, or 9), and Fe<sup>3+</sup> was added such that the final polymer concentration was 30 % and the Fe<sup>3+</sup>:catechol ratio was 2:3. Solutions were diluted with buffer until the absorbance was less than 1. Alternatively, samples were prepared by combining mPEG-cat at pH 3 for 2 h and then diluting the solutions with buffer of elevated pH.

### Synthesis of 8cPEGa

Each of the following components was completely dissolved in 75 mL of 1:2 DCM:DMF in succession before additional reagents were added: 8PEG-NH<sub>3</sub>Cl (10 g), DHPA (1.2x molar equiv. relative to amine), HBTU (1.2x molar equiv. relative to amine), and TEA (2.2x molar equiv. relative to amine). The reaction proceeded for 1.5 h at room temperature. Purification consisted of several precipitations (acidified diethyl ether at -20 °C, acidified methanol at -20 °C, methanol at -20 °C), centrifugation, and decantation. The catechol-modified PEG was vacuum dried overnight to remove residual solvent, dissolved in 12 mM HCl, filtered, transferred into dialysis tubing (3500 MWCO), and dialyzed against acidic water (pH 3.5 – 4.0) for 24 h. The material was then dialyzed against Nanopure H<sub>2</sub>O for ~3 h to minimize residual acid. The final product, 8cPEGa, was frozen and lyophilized to a white solid (~90 % conjugation).

### Hydrogel Formation

8cPEGa (50 mg) was added to 260.4 μL of Nanopure H<sub>2</sub>O of water or buffer. After complete dissolution of the polymer, 62.4 μL of 100 mM, 200 mM, or 300 mM FeCl<sub>3</sub> were added to the PEG solution in order to obtain Fe<sup>3+</sup>:catechol ratios of 1:3, 2:3, and 3:3, respectively. Gelation times were calculated by the inversion method.

### Oscillatory Rheometry

Rheometry was performed on an Anton Paar MCR 300 rheometer at 20 °C with a CP 25-2 fixture (25 mm, 2° cone angle). Solutions of 8cPEGa and Fe<sup>3+</sup> were mixed as above and added as a liquid onto the rheometer baseplate. The fixture was brought down into contact with the gel precursor liquid as quickly as possible. Time tests were performed at 100 Pa shear stress and 10 rads/s. Frequency sweeps were performed at 10 % strain from 100 rads/s to 0.1 rads/s. Step strain experiments were performed at 20 % strain, and the stress was monitored for ~300 s. Strain sweeps were performed at 10 rads/s from 1 % to 1000 % strain.

### Stability of Gels in Aqueous Environments

Gels were formed in buffers (as above) and allowed to cure for 1.5 h. Samples were submerged in 10 mL of either water or 100 mM EDTA at pH 5. After 24 h, the samples were visually examined in order to determine their stability.

### Hydrogel Formation Based on Mussel Processing

Materials were designed by adding 8cPEGa (300 mg) to 1562.4 μL of buffer at pH 3. After complete dissolution of the polymer, 374.4 μL of 200 mM FeCl<sub>3</sub> was added to the PEG



solution in order to obtain a  $\text{Fe}^{3+}$ :catechol ratio of 2:3. The solution was quickly added to 4 wells of a polytetrafluoroethylene mold in order to make cylindrical samples. After cross-linking for 24 h, the gels were swelled in 10 mL of buffer (pH 3, 5, 7, or 9) while shaking. After swelling for 24 h, the samples were ready for mechanical testing. This process was repeated in order to create the desired number of samples.

### Swelling of “Mussel-Processed” Hydrogels

Swelling experiments were performed by forming samples at pH 3 with a  $\text{Fe}^{3+}$ :catechol ratio of 2:3. Samples were weighed and swelled in buffer (pH 3, 5, 7, or 9) for 24 h at room temperature while shaking. After removing surface water, the aqueous swelling (AS) was calculated by

$$AS = \frac{m_f - m_i}{m_i} \times 100 \quad (1)$$

where  $m_i$  and  $m_f$  represent the initial and final mass of the hydrogels, respectively. Three trials were performed and the average was reported.

### Compressive Testing of “Mussel-Processed” Gels

Two types of compression tests were conducted on a Sintech 20/G mechanical tester. Relaxation experiments were performed with a 250-g load cell on cylindrical samples at a crosshead speed of 40 mm/min at room temperature. Samples were strained 5 %, 10 %, or 20 %, and the stress was monitored for 100 s. Steady-state moduli were calculated by

$$\text{Modulus} = \frac{\alpha_{100}}{\epsilon_{100}} \quad (2)$$

where  $\alpha_{100}$  and  $\epsilon_{100}$  represent the stress and strain at 100 s, respectively. The extent of relaxation was calculated by

$$\text{Relaxation} = \frac{\alpha_m - \alpha_{100}}{\alpha_m} \times 100 \quad (3)$$

where  $\alpha_m$  and  $\alpha_{100}$  represent the maximum stress and stress at 100 s, respectively. The relaxation time was calculated by

$$\sigma(t) = A_1 + A_2 \exp[-(t/\tau)^\alpha] \quad (4)$$

using MATLAB, where  $\sigma(t)$  is the stress at time  $t$  (Pa),  $A_1$  is the steady-state stress,  $A_2$  is the relaxing stress (Pa),  $t$  is the time (s),  $\tau$  is the relaxation time (s), and  $\alpha$  is the expansion coefficient. Three trials were performed, and the average values were reported.

Hysteresis experiments were performed with a 50-lb load cell on cylindrical samples at a crosshead speed of 10 mm/min at room temperature. Samples were strained to 10 %, 20 %, 40 %, 60 %, 70 %, and 80 % with a 30-s dwell each time the strain returned to 0 %.

### Supplementary Material

Refer to Web version on PubMed Central for supplementary material.

### Acknowledgments

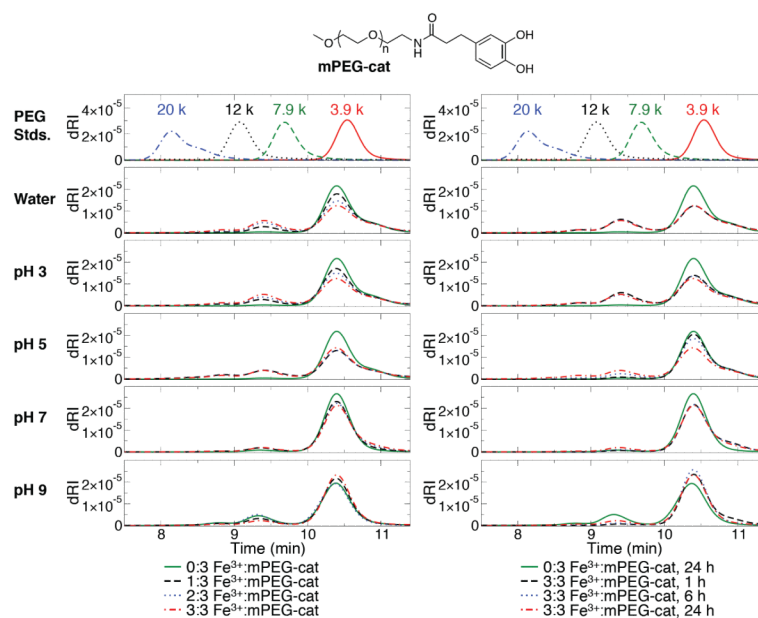
DGB and DEF contributed equally. The authors thank Dr. Wesley Burghardt, Dr. Sungjin Park, Mark Seniw, and Corey Janczak for insightful discussions. GPC experiments were performed at Northwestern University's KECK

Biophysics facility. Compression experiments made use of Central Facilities supported by the MRSEC program of the National Science Foundation (DMR-0520513) at the Northwestern University Materials Research Science and Engineering Center. This work was supported by grants from the NIH. DGB and DEF were partially supported by the IBNAM-Baxter Early Career Development Award in Bioengineering and a NIH National Research Service Award from the National Heart, Lung, and Blood Institute (F30HL096292), respectively. N.H.A. thanks the Danish Council for Independent Research, Natural Sciences for a Post-Doctoral Fellowship (No. 272-08-00087), and the University of Chicago Materials Research Science and Engineering Center (DMR 0820054) for the Kadanoff-Rice Postdoctoral Fellowship (2010-12). KYCL acknowledges support from the University of Chicago Materials Research Science and Engineering Center (DMR 0820054) and grant from the NSF (MCB-0920316). Supporting Information is available online from Wiley InterScience or from the author.

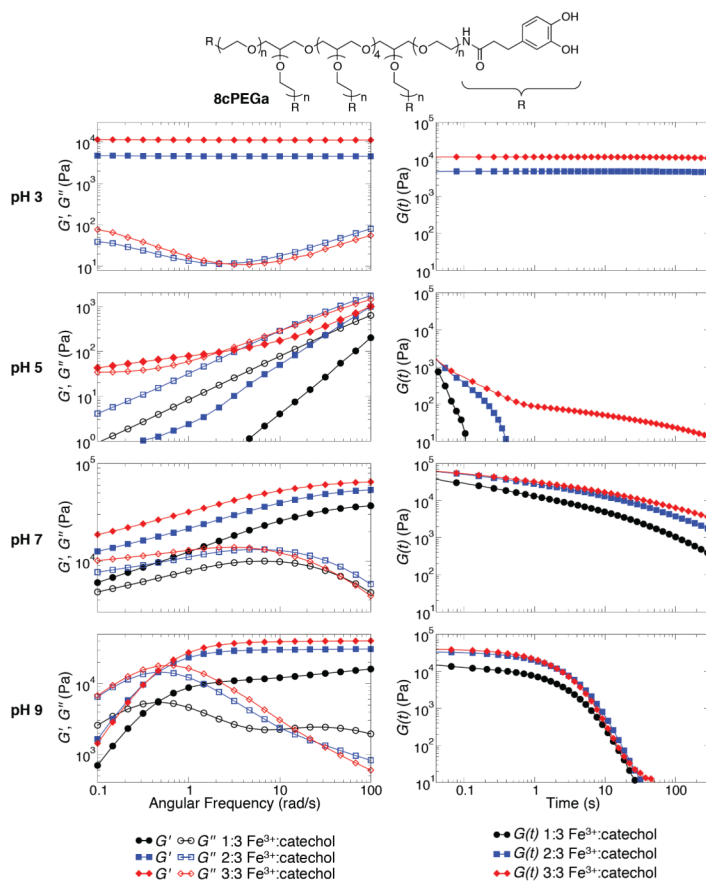
## References

- [1]. Espinosa HD, Rim JE, Barthelat F, Buehler MJ. *Prog Mater Sci.* 2009; 54:1059.
- [2]. Huebsch N, Mooney DJ. *Nature.* 2009; 462:426. [PubMed: 19940912]
- [3]. Liu K, Jiang L. *Nano Today.* 2011; 6:155.
- [4]. Antonietti M, Fratzl P. *Macromol Chem Phys.* 2010; 211:166.
- [5]. Fratzl P. *J R Soc Interface.* 2007; 4:637. [PubMed: 17341452]
- [6]. Vincent JFV. *J Mater Res.* 2008; 23:3140.
- [7]. Kluge JA, Rabotyagova O, Leisk GG, Kaplan DL. *Trends Biotechnol.* 2008; 26:244. [PubMed: 18367277]
- [8]. Lee BP, Messersmith PB, Israelachvili JN, Waite JH. *Annu Rev Mater Res.* 2011; 41:99. [PubMed: 22058660]
- [9]. Heim M, Keerl D, Scheibel T. *Angew Chem Int Ed.* 2009; 48:3584.
- [10]. Jin H-J, Kaplan DL. *Nature.* 2003; 424:1057. [PubMed: 12944968]
- [11]. Vollrath F, Knight DP. *Nature.* 2001; 410:541. [PubMed: 11279484]
- [12]. Vollrath F, Knight DP, Hu XW. *Proc R Soc B Biol Sci.* 1998; 265:817.
- [13]. Exler JH, Hümmerich D, Scheibel T. *Angew Chem Int Ed.* 2007; 46:3559.
- [14]. Rammensee S, Slotta U, Scheibel T, Bausch AR. *Proc Natl Acad Sci USA.* 2008
- [15]. Stewart RJ, Ransom TC, Hlady V. *J Polym Sci B Polym Phys.* 2011; 49:757. [PubMed: 21643511]
- [16]. Deming TJ. *Curr Opin Chem Biol.* 1999; 3:100. [PubMed: 10021411]
- [17]. Lee H, Scherer NF, Messersmith PB. *Proc Natl Acad Sci USA.* 2006; 103:12999. [PubMed: 16920796]
- [18]. Waite JH. *Int J Adhes Adhes.* 1987; 7:9.
- [19]. Vaccaro E, Waite JH. *Biomacromolecules.* 2001; 2:906. [PubMed: 11710048]
- [20]. Zhao H, Waite JH. *Biochemistry.* 2006; 45:14223. [PubMed: 17115717]
- [21]. Harrington MJ, Waite JH. *J Exp Biol.* 2007; 210:4307. [PubMed: 18055620]
- [22]. Yu J, Wei W, Danner E, Ashley RK, Israelachvili JN, Waite JH. *Nat Chem Biol.* 2011; 7:588. [PubMed: 21804534]
- [23]. Coombs TL, Keller PJ. *Aquat Toxicol.* 1981; 1:291.
- [24]. Harrington MJ, Masic A, Holten-Andersen N, Waite JH, Fratzl P. *Science.* 2010; 328:216. [PubMed: 20203014]
- [25]. Ryu JH, Lee Y, Kong WH, Kim TG, Park TG, Lee H. *Biomacromolecules.* 2011; 12:2653. [PubMed: 21599012]
- [26]. Yu M, Deming TJ. *Macromolecules.* 1998; 31:4739. [PubMed: 9680407]
- [27]. Brubaker CE, Kissler H, Wang LJ, Kaufman DB, Messersmith PB. *Biomaterials.* 2010; 31:420. [PubMed: 19811819]
- [28]. Winslow BD, Shao H, Stewart RJ, Tresco PA. *Biomaterials.* 2010; 31:9373. [PubMed: 20950851]
- [29]. Claussen KU, Giesa R, Scheibel T, Schmidt H-W. *Macromol Rapid Commun.* 2012; 33:206. [PubMed: 22183983]

- [30]. Holten-Andersen N, Harrington MJ, Birkedal H, Lee BP, Messersmith PB, Lee KYC, Waite JH. *Proc Natl Acad Sci USA*. 2011; 108:2651. [PubMed: 21278337]
- [31]. Hwang DS, Zeng H, Srivastava A, Krogstad DV, Tirrell M, Israelachvili JN, Waite JH. *Soft Matter*. 2010; 6:3232. [PubMed: 21544267]
- [32]. Zeng HB, Hwang DS, Israelachvili JN, Waite JH. *Proc Natl Acad Sci USA*. 2010; 107:12850. [PubMed: 20615994]
- [33]. Anderson TH, Yu J, Estrada A, Hammer MU, Waite JH, Israelachvili JN. *Adv Mater*. 2010; 20:4196.
- [34]. Xu H, Nishida J, Ma W, Wu H, Kobayashi M, Otsuka H, Takahara A. *ACS Macro Letters*. 2012; 1:457.
- [35]. Mentasti E, Pelizzetti E. *J Chem Soc, Dalton Trans*. 1973:2605.
- [36]. Mentasti E, Pelizzetti E, Saini G. *J Chem Soc, Dalton Trans*. 1973:2609.
- [37]. Sever MJ, Weisser JT, Monahan J, Srinivasan S, Wilker JJ. *Angew Chem Int Ed*. 2004; 43:448.
- [38]. Johnson GA, Tramaglino DM, Levine RE, Ohno K, Choi N-Y, Woo SL-Y. *J Orthop Res*. 1994; 12:796. [PubMed: 7983555]
- [39]. Hayes WC, Mockros LF. *J Appl Physiol*. 1971; 31:562. [PubMed: 5111002]
- [40]. Avdeef A, Sofen SR, Bregante TL, Raymond KN. *J Am Chem Soc*. 1978; 100:5362.
- [41]. Lee BP, Dalsin JL, Messersmith PB. *Biomacromolecules*. 2002; 3:1038. [PubMed: 12217051]
- [42]. Wilker JJ. *Curr Opin Chem Biol*. 2010; 14:276. [PubMed: 20036600]
- [43]. Lv S, Dudek DM, Cao Y, Balamurali MM, Gosline J, Li H. *Nature*. 2010; 465:69. [PubMed: 20445626]
- [44]. Thompson JB, Kindt JH, Drake B, Hansma HG, Morse DE, Hansma PK. *Nature*. 2001; 414:773. [PubMed: 11742405]
- [45]. Fantner GE, Hassenkam T, Kindt JH, Weaver JC, Birkedal H, Pechenik L, Cutroni JA, Cidade GAG, Stucky GD, Morse DE, Hansma PK. *Nat Mater*. 2005; 4:612. [PubMed: 16025123]
- [46]. Rief M, Gautel M, Oesterhelt F, Fernandez JM, Gaub HE. *Science*. 1997; 276:1109. [PubMed: 9148804]
- [47]. Smith BL, Schaffer TE, Viani M, Thompson JB, Frederick NA, Kindt J, Belcher A, Stucky GD, Morse DE, Hansma PK. *Nature*. 1999; 399:761.
- [48]. Fantner GE, Oroudjev E, Schitter G, Golde LS, Thurner P, Finch MM, Turner P, Gutschmann T, Morse DE, Hansma H, Hansma PK. *Biophys J*. 2006; 90:1411. [PubMed: 16326907]
- [49]. Abdurrahmanoglu S, Can V, Okay O. *Polymer*. 2009; 50:5449.
- [50]. Zhang C, Aung A, Liao L, Varghese S. *Soft Matter*. 2009; 5:3831.
- [51]. Kushner AM, Vossler JD, Williams GA, Guan Z. *J Am Chem Soc*. 2009; 131:8766. [PubMed: 19505144]
- [52]. Tang L, Liu W, Liu G. *Adv Mater*. 2010; 22:2652. [PubMed: 20491091]
- [53]. Phadke A, Zhang C, Arman B, Hsu C-C, Mashelkar RA, Lele AK, Tauber MJ, Arya G, Varghese S. *Proc Natl Acad Sci USA*. 2012
- [54]. Xu D, Craig SL. *Macromolecules*. 2011; 44:7478. [PubMed: 22043083]

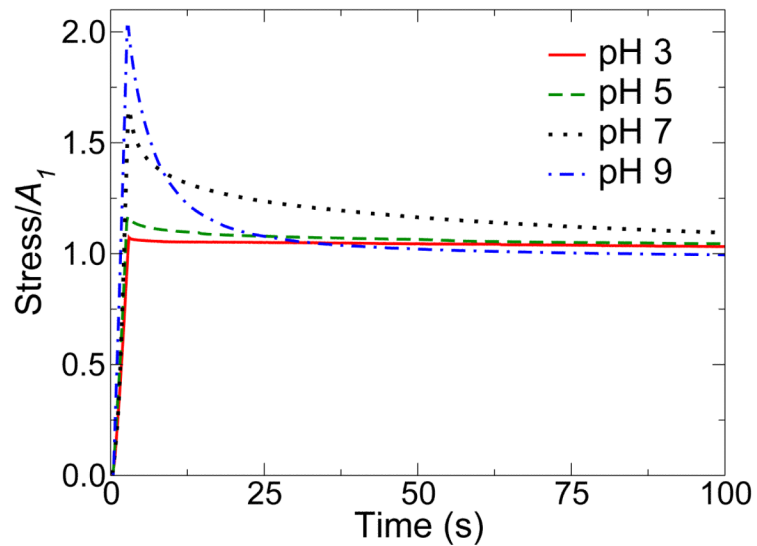


**Figure 1.** GPC data of mPEG-cat (top) after 24 h incubation with Fe<sup>3+</sup> (left) and time dependence of the reaction with Fe<sup>3+</sup> (right). Monomers and multimers elute at ~10-11 min and ~8.5-10 min, respectively.

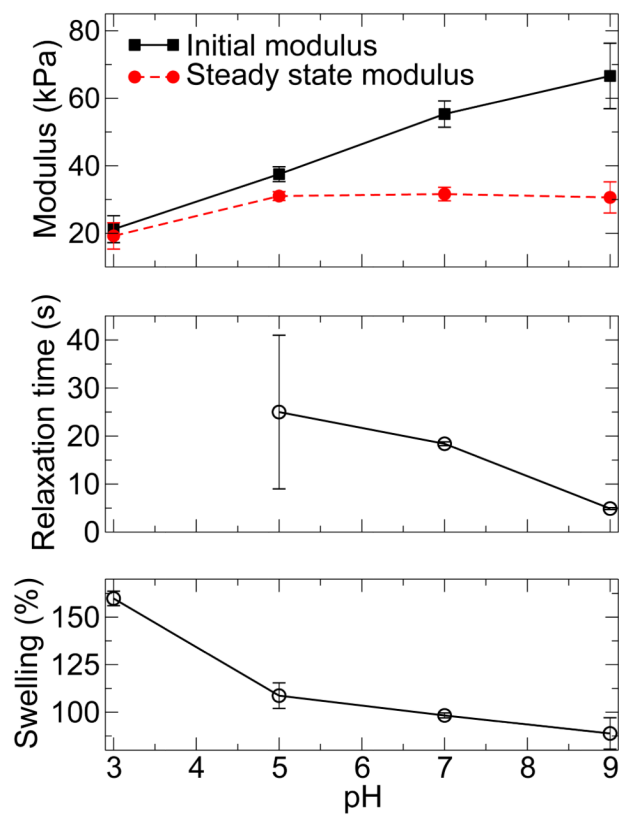


**Figure 2.** Frequency sweep (left) and step strain (right) characterizations of hydrogels composed of 8cPEGa (top) and Fe<sup>3+</sup> at pH 3, 5, 7, and 9.

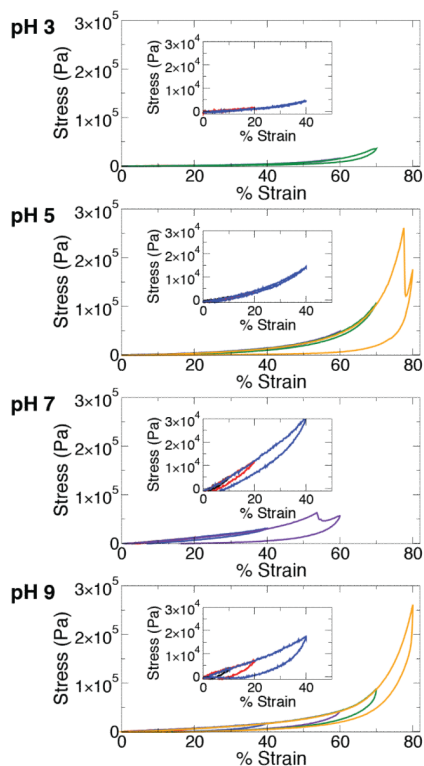




**Figure 3.** pH-dependent relaxation of mussel inspired hydrogels containing covalent and coordination bonds. Samples were formed at pH 3 and then equilibrated to the pH values indicated before testing in compression. Samples were strained to 20 %, and the stress was monitored for 100 s.  $A_1$  represents the steady-state stress.

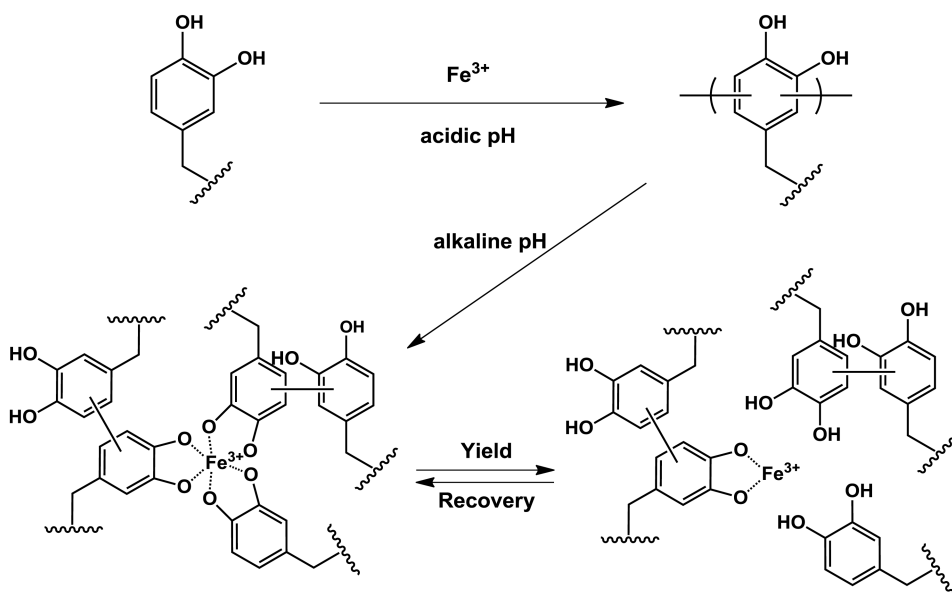


**Figure 4.** Physical characterization of mussel inspired gels formed at pH 3 and then equilibrated at pH 3-9. Initial and steady-state moduli demonstrate pH-dependent differences due to the presence of coordination bonds and their ability to dissipate energy (top panel). Relaxation times (center panel) and swelling (bottom panel) decrease with increasing pH. The relaxation time for gels both formed and equilibrated at pH 3 is not shown, as it was essentially infinite.



**Figure 5.**

Representative stress-strain curves of gels formed by mussel-mimetic processing involving initial cross-linking at pH 3 and then equilibration to the pH values indicated. Samples were deformed in multiple compression cycles, where the strain was successively increased to 10 % (black), 20 % (red), 40 % (blue), 60 % (purple), 70 % (green), and 80 % (yellow). In the case of materials equilibrated at pH 7, the final two loops were unnecessary due to failure at ~55 % strain. Insets show detail in the low strain regime (0-50%).

**Scheme 1.**

Proposed pH dependence of covalent and coordination bond formation in catechol polymer hydrogels containing  $\text{Fe}^{3+}$ . Reaction of catechol-terminated branched PEG with  $\text{Fe}^{3+}$  at acidic pH results in covalently cross-linked hydrogels. Subsequent equilibration of these gels at pH 5, 7, or 9 introduces varying amounts of  $\text{Fe}^{3+}$ -catechol coordination bonds that mechanically enhance the covalent network. Under the influence of a mechanical force, these coordination bonds reversibly rupture and re-form, acting as a mechanism for energy dissipation. Both oligomeric and monomeric (unreacted) catechols are believed to participate in the coordination network.